ECCM21

02-05 July 2024 | **Nantes - France**

Proceedings of the 21st European Conference on Composite Materials

Vol 8

Special Sessions

WWW.ECCM21.ORG

UNDER THE PATRONAGE OF:

ESCM European Society For Composite Materials

Association pour les MAtériaux Composites AMAC

EuCIA The European Voice of Composites

WITH THE SUPPORT OF:

RÉGION PAYS DE LA LOIRE

ORGANIZED BY:

CENTRALE NANTES

Nantes Université

SUPPORTING PARTNER:

JEC CONNECTING THE WORLD WITH COMPOSITES

Edited by:

Prof. Christophe BINETRUY
ECCM21 Conference Chair
Institute of Civil Engineering and Mechanics (GeM)
Centrale Nantes
Nantes Université

Prof. Frédéric JACQUEMIN
ECCM21 Conference Co-Chair
Institute of Civil Engineering and Mechanics (GeM)
Nantes Université

Published by:

The European Society for Composite Materials (ESCM) and the Ecole Centrale de Nantes.

These Proceedings have an ISBN (owned by the Publisher) and a DOI (owned by the Ecole Centrale de Nantes).

ISBN: 978-2-912985-01-9
DOI: 10.60691/yj56-np80

Disclaimer:

Editorial

This collection contains the proceedings of the 21st European Conference on Composite Materials (ECCM21), held in Nantes, France, July 2-5, 2024. ECCM21 is the 21st in a series of conferences organized every two years by the members of the European Society of Composite Materials (ESCM). As some of the papers in this collection show, this conference reaches far beyond the borders of Europe.

The ECCM21 conference was organized by the Nantes Université and the Ecole Centrale de Nantes, with the support of the Research Institute in Civil and Mechanical Engineering (GeM).

Each volume gathers contributions on specific topics:

- **Vol 1. Industrial applications**
- **Vol 2. Material science**
- **Vol 3. Material and Structural Behavior – Simulation & Testing**
- **Vol 4. Experimental techniques**
- **Vol 5. Manufacturing**
- **Vol 6. Multifunctional and smart composites**
- **Vol 7. Life cycle performance**
- **Vol 8. Special Sessions**

Nantes, the birthplace of the novelist Jules Verne, is at the heart of this edition, as are the imagination and vision that accompany the development of composite materials. They are embodied in the work of numerous participants from the academic world, but also of the many industrialists who are making a major contribution to the development of composite materials. Industry is well represented, reflecting the strong presence of composites in many application areas.

With a total of 1,064 oral and poster presentations and over 1,300 participants, the 4-day event enabled fruitful exchanges on all aspects of composites. The topics that traditionally attracted the most contributions were fracture and damage, multiscale modeling, durability, aging, process modeling and simulation and additive manufacturing.

However, the issues of energy and environmental transition, and more generally the sustainability of composite solutions, logically appear in this issue as important contextual elements guiding the work being carried out. This includes bio-sourced composites, material recycling and reuse of parts, the environmental impact of solutions, etc.

We appreciated the high level of research presented at the conference and the quality of the submissions, some of which are included in this collection. We hope that all those interested in the progress of European composites research in 2024 will find in this publication sources of inspiration and answers to their questions.

Prof. Christophe BINETRUY
ECCM21 Conference Chair
Institute of Civil Engineering
and Mechanics (GeM)
Centrale Nantes
Nantes Université

Prof. Frédéric JACQUEMIN
ECCM21 Conference Co-Chair
Institute of Civil Engineering
and Mechanics (GeM)
Nantes Université

Under the Patronage of:

ESCM European Society For Composite Materials

Association pour les AMAC MAtériaux Composites

EuCIA The European Voice of Composites

Organized by: CENTRALE NANTES — Nantes Université

With the support of: RÉGION PAYS DE LA LOIRE

Supported by: EMC2 — JEC CONNECTING THE WORLD WITH COMPOSITES

Sponsored by:

Bronze Partner: BRUKER — INSTRON — MatchID Metrology beyond colors

Other partners: CAPACITÉS De la recherche à l'innovation — CARBON AXIS — CETIM

Depestele — EikoSim — ELSEVIER — FAIRMAT

metravib material testing — NOVITOM — Quantiflex simulations — Surface Measurement Systems World Leader in Sorption Science

Hosting Organizations

Conference chairs

Prof. Christophe BINETRUY
ECCM21 Conference Chair
Institute of Civil Engineering and Mechanics (GeM)
Centrale Nantes
Nantes Université

Prof. Frédéric JACQUEMIN
ECCM21 Conference Co-Chair
Institute of Civil Engineering and Mechanics (GeM)
Nantes Université

International Scientific Committee

Malin Akermo (Sweden)
Remko Akkerman (Netherlands)
Andrey Aniskevich (Latvia)
Leif Asp (Sweden)
Emmanuel Baranger (France)
Janice Barton (UK)
Johnny Beaugrand (France)
Andrea Bernasconi (Italy)
Christophe Binetruy (France)
Thomas Bohlke (Germany)
Alain Bourmaud (France)
Nicolas Boyard (France)
Joël Breard (France)
Richard Butler (UK)
Baris Caglar (Netherlands)
Pedro Camanho (Portugal)
Pierpaolo Carlone (Italy)
Paolo Andrea Carraro (Italy)
Valter Carvelli (Italy)
Nuno Correia (Portugal)
Gergely Czél (Hungary)
Clemens Dransfeld (Netherlands)
Sylvain Drapier (France)
Klaus DRECHSLER (Germany)
Andreas ECHTERMEYER (Norway)
Paolo Ermanni (Switzerland)
Martin Fagerström (Sweden)
Ewald Fauster (Austria)
Julien Ferec (France)
Antonio Ferreira (Portugal)
Bodo Fiedler (Germany)
Stefanos Giannis (UK)
Nathalie Godin (France)
Carlos Gonzalez (Spain)
Sotirios Grammatikos (Norway)
Christoph Greb (Germany)
Emile Greenhalgh (UK)
Gianmarco Griffini (Italy)
Stephen Hallett (UK)
Nahiene Hamila (France)
Roland Hinterhoelzl (Austria)
Martin Hirsekorn (France)
Darko Ivančević (Hungary)
Frédéric Jacquemin (France)
Mikko Kanerva (Finland)
Luise Karger (Germany)
Vassilis Kostopoulos (Greece)
Theodosia Kourkoutsaki (Germany)
Thomas Kruse (Germany)
Ugo Lafont (France)
Jacques Lamon (France)
Frédéric Laurin (France)
Antoine Le Duigou (France)
Stepan Lomov (Belgium)
Theodoros Loutas (Greece)
Staffan Lundstrom (Sweden)
António Marques (Portugal)
David May (Germany)
Véronique Michaud (Switzerland)
Jörg Mussig (Germany)
Thomas Neumeyer (Germany)
Philippe Olivier (France)
Alkiviadis Paipetis (Greece)
Federico Paris (Spain)
Chung Hae Park (France)
John-Alan Pascoe (Netherlands)
Alessandro Pegoretti (Italy)
Ton Peijs (UK)
Rob Pierce (Denmark)
Soraia Pimenta (UK)
Silvestre Pinho (UK)
Gerald Pinter (Austria)
Connie Qian (UK)
Marino Quaresimin (Italy)
Andrew Rhead (UK)
Paul Robinson (UK)
Essi Sarlin (Finland)
Yentl Swolfs (Belgium)
Sofia Teixeira du Freitas (Netherlands)
Julie Teuwen (Netherlands)
Ole Thomsen (UK)
Stavros Tsantzalis (Greece)
Konstantinos Tserpes (Greece)
Albert Turon (Spain)
Julien van Campen (Netherlands)
Wim Van Paepegem (Belgium)
Anastasios Vassilopoulos (Switzerland)
Ignaas Verpoest (Belgium)
Michael Wisnom (UK)
Dimitrios Zarouchas (Netherlands)
Daiva Zeleniakiene (Lithuania)
Dan Zenkert (Sweden)

Local Organizing Committee

Suresh Advani
Romain Agogué
Sylvain Chataigner
Sébastien Comas-Cardona
Sofiane Guessasma
Suzanne Laïk
Philippe Le Bot
Mael Peron
Luisa Silva
Vincent Sobodka
Alexandre Ripoche
Elena Syerko

X

Table of Contents

DETERMINING THE UNDERLYING MICROSTRUCTURAL FEATURES INITIATING COMPRESSIVE FAILURE IN FIBRE REINFORCED POLYMERS

H.L. Khoo[1,2*], R. Trask[3], S. Pimenta[1], and P. Robinson[2]

[1]Department of Mechanical Engineering, Imperial College London, London, UK
[2]Department of Aeronautics, Imperial College London, London, UK
[3]Bristol Composites Institute, University of Bristol. Bristol, UK
*Email : hlk18@ic.ac.uk

Keywords: Fibre reinforced polymers, compressive failure, failure initiation

Abstract
Microstructural features governing FRP compressive failure initiation were identified by analysing computational simulations of 2D FRP microstructures with random fibre waviness. Results showed that failure initiation was not governed by magnitude of fibre misalignment angle (θ_f) but rather by the pattern or spatial variation of $\theta_{f,}$ as well as fibre volume fraction (V_f). This finding remained consistent regardless of changes to FRP microstructural parameters.

1. Introduction

The industrial popularity of fibre reinforced polymers (FRPs), for example in aerospace and medicine, can be attributed to their range of attractive properties including high specific strength and stiffness [1]. However, FRPs are notably limited by their compressive performance. A considerable challenge in addressing this limitation is the understanding of factors that initiate or promote FRP compressive failure. In existing literature [2,3], much attention has been given to exploring the effect of fibre misalignment (θ_f) on FRP compressive strength, and the negative correlation between them has been well established. Some studies [3] suggest that maximum misalignment angle ($\theta_{f,max}$) is an accurate predictor for FRP compressive strength, implicating θ_f magnitude as the main factor initiating compressive failure. However, there is evidence that other FRP microstructure parameters, such as the spatial variation of fibre misalignment within the composite, could also play a significant role [3,4].

This work aims to uncover the underlying microstructural features that initiate FRP compressive failure through systematic variation of FRP microstructural parameters, implemented through variation of fibre misalignment field. Parameters varied include fibre misalignment field correlation length (length over which the field's autocorrelation function reduces to 0.1), model size, and mean fibre misalignment angle $\overline{\theta_f}$. All θ_f fields result in random fibre waviness. Through computational simulation of the behaviour of 2D FRP microstructures under compressive load, the microstructural features common to the critical region surrounding the failure initiation site were highlighted.

2. Method

2.1. Generation of fibre misalignment angle field

The fibre misalignment angle field generation method begun with the definition of a 2D power spectral density (PSD) function:

$$PSD = S_o \exp\left[-\left(\frac{w_x}{w_{0x}}\right)^2 - \left(\frac{w_y}{w_{0y}}\right)^2\right] \quad (1)$$

where w are spatial frequencies (with units of 1/µm), and subscripts denote frequency along (x) or transverse (y) to the fibre direction. S_o, w_{0x}, w_{0y} are tuning variables used to achieve the fibre misalignment field variations summarised in Table 1 (baseline values are representative of prepreg CFRPs [4]). All fields have a θ_f standard deviation of 1.15°.

From the defined PSD, signal processing theory [4] was then used to transform the 2D PSD function to a 2D signal, which generated stochastic fibre misalignment angle θ_f fields (Figure 1); this allowed many random realisations of θ_f fields to be generated with the same PSD.

The fibres have a diameter $\phi_f = 7$ µm, and the FRP has a fibre volume fraction $V_f = 60\%$ assuming 3D hexagonal packing; the 2D models represent one of the FRP symmetry planes where the interfibre distance is minimised (8.61 µm on average). The θ_f fields represent each fibre individually, with a resolution in the fibre longitudinal direction of $3.5\phi_f = 24.5$ µm. Exponential fading of misalignment angle was applied as an extension of each fibre, to minimise initiation of edge failures [5].

Table 1. FRP fibre misalignment field variations.

Variation	Number of random realisations	$\overline{\theta_f}$ (°)	Model Size (µm) Length L	Model Size (µm) Height H	Correlation Length (µm) Longitudinal $l_x = w_{0x}^{-1}/2$	Correlation Length (µm) Transverse $l_x = w_{0y}^{-1}/2$
Baseline	250	1.50	7938	7921	1350	730
M1	100	0.75	7938	7921	1350	730
M2	100	3.00	7938	7921	1350	730
S1	100	1.50	5586	5579	1350	730
S2	100	1.50	11221	11193	1350	730
C1	100	1.50	7938	7921	1080	580
C2	100	1.50	7938	7921	1690	910

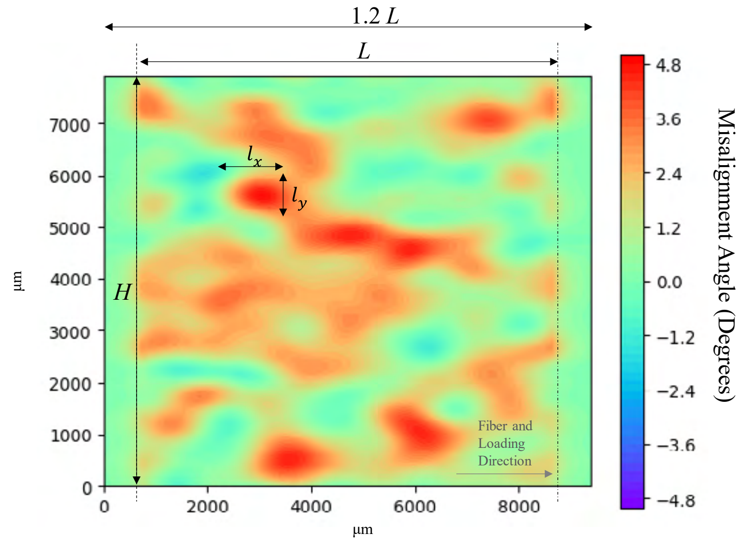

Figure 1. Typical contour plot of fibre misalignment angle θ_f field (baseline variation).

Each θ_f field was then used to define a 2D FRP microstructure; the minimum matrix layer height was kept constant across all adjacent fibers. A corresponding fibre volume fraction (V_f) field was calculated for each FRP microstructure to capture local changes in fibre volume fraction.

2.2. Computational simulation

The defined 2D FRP microstructures were created computationally in Abaqus and loaded in compression using Riks analysis. Element size followed the resolution of the θ_f fields. The orthotropic carbon-fibres and non-linear elastic-plastic epoxy-matrix were modelled using plane strain elements with reduced integration and hourglass control.

For each FRP simulation, the global stress-strain behaviour, as well as the plastic strain distribution at peak global stress was extracted. The FRP's failure initiation site was subsequently defined as the location exhibiting highest plastic strain when the FRP reaches peak global stress.

2.3. Post-processing

To identify microstructural features common to the failure initiation sites, for each θ_f field variation, the following averaging process was used (Figure 2) [6]:

1. For each random FRP realisation, redefine its origin as its failure initiation site.
2. Superimpose all fibre misalignment angle fields by aligning their redefined origins.
3. Average all fields through the number of random realisations.
4. Repeat steps 2-3 for the FRPs' V_f fields.

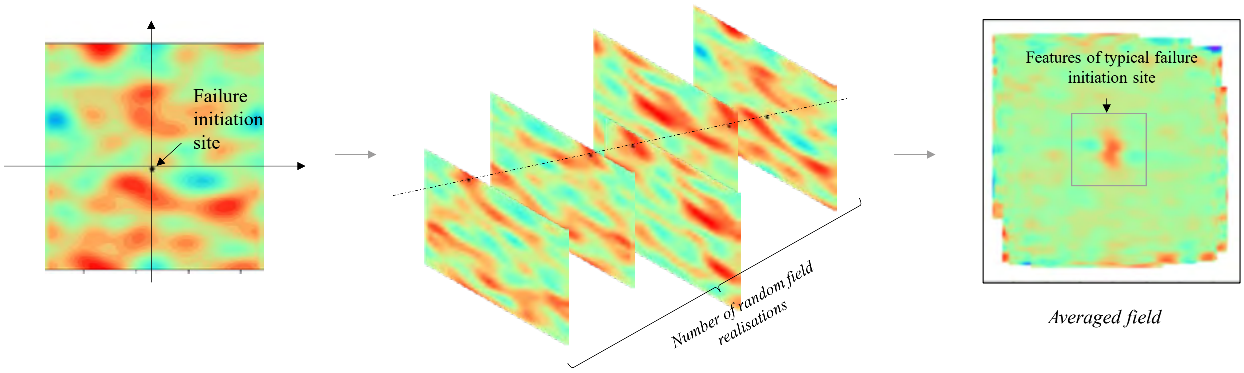

Figure 2. Steps 1 to 3 of FRP θ_f field averaging process.

3. Results

3.1. Typical failure initiation site features

The averaged fibre misalignment angle and volume fraction fields (Figures 3a and 3b) show that FRP compressive failure initiation tends to occur in regions of high fibre misalignment as well as fibre volume fraction. This remained true for all FRP variations explored.

The region of high fibre misalignment containing the failure initiation site extends transverse to the fibre direction. In fibre path terms, this indicates a region where many neighbouring fibres are locally misaligned in-phase. Interestingly, the averaged θ_f field shows regions of significantly lower θ_f on either side of the high θ_f region where failure initiates. This suggests that compressive failure also tends to localise at regions with sharp changes in fibre misalignment angle along the fibre direction. In an industrial setting, this would be particularly evident in components involving ply-drops or localised wrinkles (e.g. due to surface curvature) [7].

CONTENTS

The identified pattern of high and low θ_f surrounding the failure initiation site inherently gives rise to a region of high V_f, as reflected in the averaged V_f field. For regions with high V_f, or thin local matrix layer, less energy would be needed for the local matrix region to experience high shear strains and undergo unstable shear deformation (resulting in failure localisation) in comparison to other regions with comparable fibre misalignment angle but lower V_f. Hence, it is suggested that high V_f is not simply a result of the θ_f pattern identified but is also a preferred characteristic of failure initiation sites.

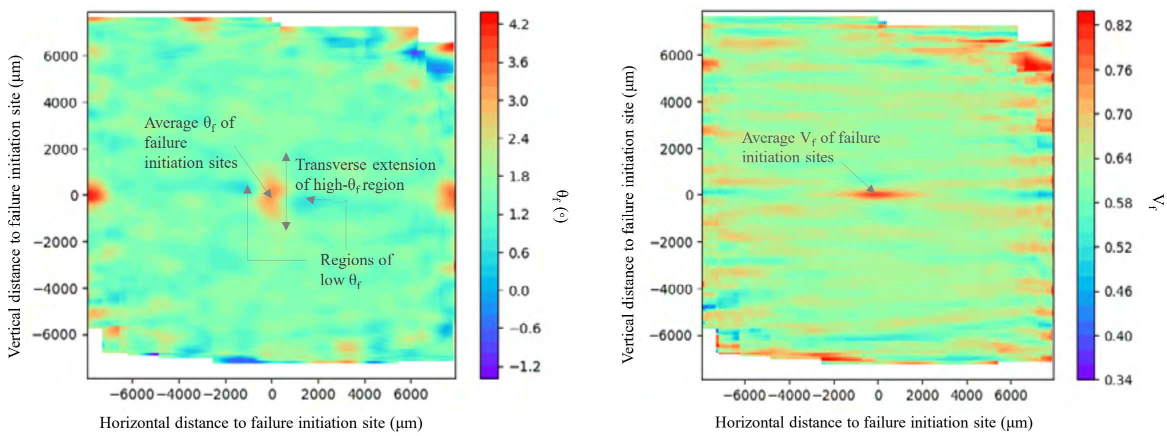

(a) θ_f (b) V_f

Figure 3. Averaged features of FRP compressive failure initiation site (baseline variation).

To verify that the fibre misalignment pattern identified is unique to failure initiation sites and not an inherent property of high-θ_f regions within the fibre misalignment fields generated, the same averaging process (as described in 2.3) was conducted with the redefined origin set as the global maxima of the θ_f fields instead. The averaged fibre misalignment angle field in this case (Figure 4) reflects the typical features of high-θ_f angle regions within the defined fibre misalignment angle fields.

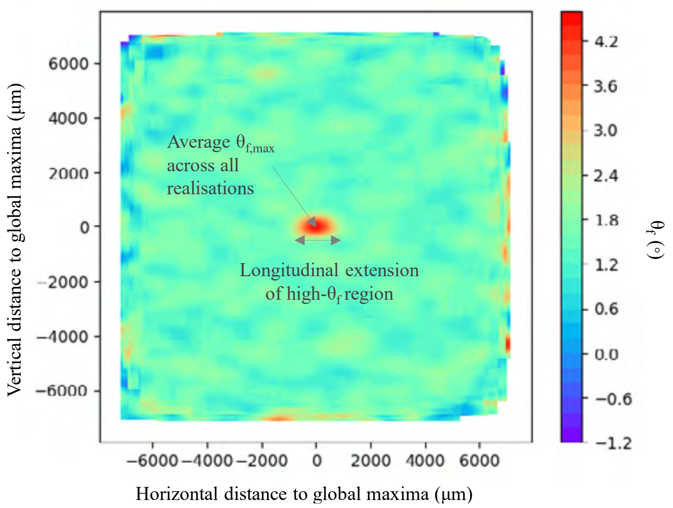

Figure 4. Averaged features of FRP high-θ_f region (baseline variation).

Comparing Figure 3a to Figure 4, in terms of fibre misalignment angle distribution, the typical high-θ_f region in FRPs is in stark contrast to the typical failure initiation site. Figure 4 clearly shows a high fibre misalignment region that extends along the fibre direction, reflecting the ratio of correlation lengths defined in Table 1.

Note that if FRPs were assumed to fail at the location of maximum θ_f, Figures 3a and 4 should be similar. With their strong dissimilarity, it is clear that fibre misalignment angle alone does not govern FRP compressive failure initiation.

3.2. Average θ_f and V_f of failure initiation sites

In general, the changes in average θ_f and V_f of failure initiation sites between variations follow changes in maximum values (i.e. $\theta_{f,max}$ and $V_{f,max}$) of the respective fields (Figures 5a and 5b).

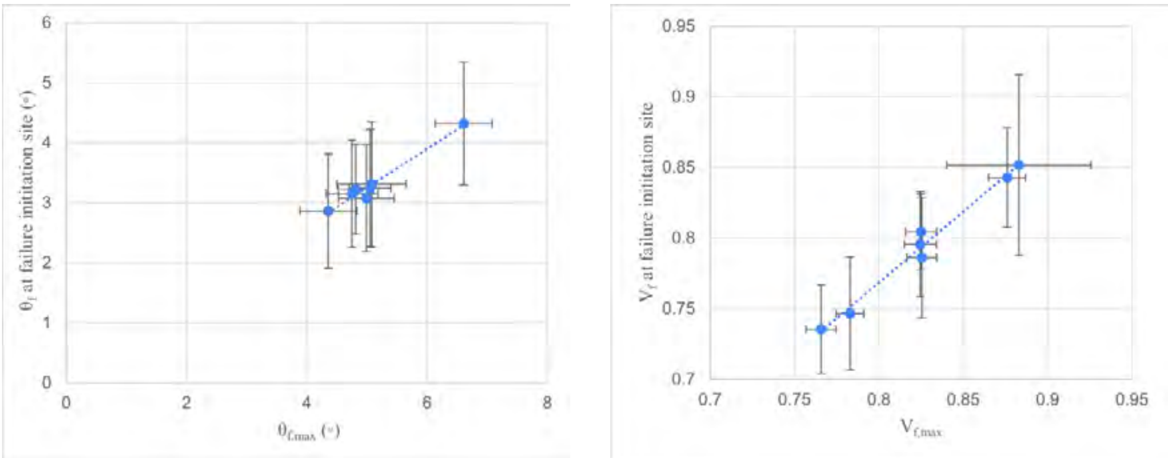

(a) θ_f (b) V_f

Figure 5. The relationship between θ_f,V_f of failure initiation sites and $\theta_{f,max}$,$V_{f,max}$ across FRP microstructure variations explored.

3.3. FRP compressive strength

Table 2. FRP compressive strength.

Variation	$\overline{\theta_f}$ (∘)	Compressive strength (MPa)
Baseline	1.50	986 ± 45
M1	0.75	1264 ± 75
M2	3.00	679 ± 26
S1	1.50	1009 ± 49
S2	1.50	986 ± 54
C1	1.50	988 ± 48
C2	1.50	997 ± 58

All variations with the same $\overline{\theta_f}$ exhibited similar compressive strengths (Table 2). As expected from existing micromechanical models [3,8], there is an inverse relationship between mean misalignment angle and compressive strength. Interestingly, increasing the correlation length of the fibre misalignment field (i.e. the size of the typical high fibre misalignment angle region) had a negligible effect on FRP compressive strength.

4. Conclusions

It is evident that spatial distribution of fibre misalignment angle is a key predictor of FRP compressive failure initiation location. Local magnitudes of fibre volume fraction and misalignment angle are also of importance. Overall, failure initiation of FRPs cannot be identified purely based on the maxima of the fibre misalignment field but rather must consider the local spatial variation of neighboring regions and fibre volume fraction as well.

Acknowledgments
The authors would like to acknowledge the funding for this research provided by UK Engineering and Physical Sciences Research Council (EPSRC) programme Grant EP/T011653/1. Next Generation Fibre-Reinforced Composites: a Full Scale Redesign for Compression in collaboration with University of Bristol.

References

[1] J. Zhang, G. Lin, U. Vaidya, and H. Wang. Past, present and future prospective of global carbon fibre composite developments and applications. *Composites Part B*, 250, 2022.
[2] G. Zhang and R.A. Latour. FRP Composite Compressive Strength and Its Dependence upon Interfacial Bond Strength, Fiber Misalignment, and Matrix Nonlinearity. *Journal of Thermoplastic Composite Materials*, 6(4):298–311, 1993.
[3] D. Wilhelmsson, R. Gutkin, F. Edgren, and L.E. Aspa. An experimental study of fibre waviness and its effects on compressive properties of unidirectional NCF composites. *Composites Part A.,* 107:665–674, 2018.
[4] D. Liu, N.A. Fleck, and M.P.F. Sutcliffe. Compressive strength of fibre composites with random fibre waviness. *Journal of the Mechanics and Physics of Solids*, 52:1481 – 1505, 2004.
[5] Sutcliffe MPF. Modelling the effect of size on compressive strength of fibre composites with random waviness. *Composites Science and Technology*. 142–50. 2013.
[6] T.W.J. de Geus, R.H.J. Peerlings, and M.G.D. Geers. Microstructural topology effects on the onset of ductile failure in multi-phase materials – a systematic computational approach. *International Journal of Solids and Structures,* 67-68, 2015.
[7] Kulkarni, P., Mali, K.D. and Singh, S. An overview of the formation of fibre waviness and its effect on the mechanical performance of Fibre Reinforced Polymer Composites, *Composites Part A: Applied Science and Manufacturing*, 137, 2020.
[8] Wisnom, M.R. The effect of fibre misalignment on the compressive strength of unidirectional carbon fibre/epoxy, *Composites, 21*(5), pp. 403–407. 1990.

ECCM21

02-05 July 2024 | **Nantes - France**

Volume 8

Special Sessions

ISBN: 978-2-912985-01-9
DOI: 10.60691/yj56-np80